Progress in Organic Coatings 161 (2021) 106510

Contents lists available at ScienceDirect

Progress in Organic Coatings

journal homepage: www.elsevier.com/locate/porgcoat

Corrosion protection of brown and green patinated bronze

Tadeja Kosec [a,*], Živa Novak [a], Erika Švara Fabjan [a], Luka Škrlep [a], Andrijana Sever Škapin [a], Polonca Ropret [b,c]

[a] Slovenian National Building and Civil Engineering Institute, Dimičeva ulica 12, Ljubljana, Slovenia
[b] Research Institute, Institute for the Protection of the Cultural Heritage of Slovenia, Poljanska 40, 1000 Ljubljana, Slovenia
[c] Museum Conservation Institute, Smithsonian Institution, 4210 Silver Hill Rd., Suitland, MD 20746, United States of America

ARTICLE INFO

Keywords:
Corrosion
Protection
Bronze
Brown and green patinas
Raman and XRD analysis
SEM/EDS analysis

ABSTRACT

Bronze surfaces, whether bare or patinated, tend to change when exposed to an outdoor atmosphere. Art made of bronze which is exposed to the outdoors is usually artificially patinated. This patina changes when exposed to rain, especially in polluted rain, where sulphuric, nitric or carbonic acids are present.

In order to gain optimal protection of different patinas and consequently reduce the patina changes over the time different protection systems were developed, tested and tailored. Three types of patina (brown, green sulphate, and green persulphate) were prepared, protected and subsequently studied. The protections were based on two coatings (i) fluoropolymer based coating (FA-MS) and (ii) newly developed fluoropolymer based coating with addition of mercaptopropyl groups, named as alternative fluoropolymer coating (FA-MS-SH). Both the pure patinas applied on bronze surfaces as well as the bare bronze were electrochemically tested, first unprotected and then following the application of two different types of protection. After the protection was applied to the patinas, the change in colour was defined. Different techniques were utilised in order to define the morphology and structure of the patinas, as well as the change in colour following application of the coating. It was shown that a fluoropolymer coating (FA-MS) provided the most efficient protection to bare bronze and the sulphate patina, while a newly proposed alternative fluoropolymer coating (FA-MS-SH) offered good protection to bare and brown patinated bronze. A mechanism for the protection of bare and patinated bronze was suggested.

1. Introduction

Bronze surfaces tend to oxidize in humid air, forming red-brown cuprite, Cu_2O, which slowly further oxidizes into tenorite, CuO [1]. If these surfaces are exposed to polluted atmospheres containing sulphates, carbonates, nitrates or even chloride ions, secondary corrosion products may form, which, in most cases, do not protect bronze from further corrosion. Numerous protective methods are used to preserve patinated bronze surfaces, whether the patinas are naturally developed or artificially achieved [2]. Many well-established methods of protection are used in conservation practice, including the application of inhibitors (among which benzotriazole is most commonly used), varnishes such as Paraloid 72 and Incralac, or natural or microcrystalline waxes [2–4].

Research regarding the use of a fluoropolymer coating on copper, bronze and patinated bronze has been conducted [5,6], with weakness reported as a result of the poor adhesion of such a coating to bronze surfaces [5]. Research was carried out to improve this, by incorporating methyl methacrylate and methacryloxypropyl-trimethoxysilane (abbreviated as MS) as an adhesion promoter, which led to an excellent protection efficiency on aged bronze surfaces [7].

The protection of patinated bronze or copper has been challenging, since each patina represents a unique surface structure and morphology either naturally achieved or chemically prepared by means of artificial manipulation [8]. The production of representative patinas, used for development and validation of conservation materials, is also of a great importance [9].

A protection system suitable for the green patina found on ancient bronze, which contains carbonate and sulphate minerals, has been explored [10,11]. The most efficient protection was achieved using a 2-mercapto-5-amino-1,3,4-thiadiazole inhibitor with a nitrocellulose lacquer [11]. In a recent paper, the protection of microcrystalline, Cosmolloïd wax and HC10 was tested on century-old copper corrosion products, and it was found that the penetration depth of the coating depended on the mode of application, which subsequently affected the

* Corresponding author.
E-mail address: tadeja.kosec@zag.si (T. Kosec).

https://doi.org/10.1016/j.porgcoat.2021.106510
Received 16 June 2021; Received in revised form 27 August 2021; Accepted 30 August 2021
Available online 8 September 2021

durability of the coating [12].

One study showed that Cu-Si-Mn bronze artificially patinated using a K_2S solution was efficiently protected by a 3-mercapto-propyl-trimethoxysilane coating (PropS-SH), a non-toxic alternative to Incralac, which is usually applied to outdoor artistic bronzes [13]. Our previous research on artificially patinated surfaces has included the study of the stability of green nitrate, green chloride patina types, and electrochemically formed patinas, as well as their various methods of protection, including different inhibitors, laquers and waxes that are commonly used in restoration practice [14,15]. A special pretreatment method for the use of inhibitors was proposed, and the weakness of the use of Paraloid protection was demonstrated [14]. For a chloride type patina on bronze, L-cysteine has been reported to be an efficient inhibitor [16].

This paper explores the electrochemical behavior of a fluoropolymer type of coatings on patinated bronzes. Our approach in the scientific value of the presented study is:

1) the first aim was evaluation of previously developed fluoropolymer coating FA-MS on brown patinated bronze and two different sulphate patinas in comparison to bare bronze
2) the second aim was to develop a new fluoropolymer coating, containing mercaptosilane in order to seek possible better efficiency on brown and green patinas together with explanations for such behavior.

In our previous research work we presented the development and protection efficiency as well as mechanism of bonding of a fluoropolymer coating (FA-MS) applied on aged bronze representing archaeological bronze [7]. We have shown the FA-MS coating continuously covered the surface of the patinated/aged bronze and showed very good inhibition efficiency. In this paper, the application of a fluoropolymer coating (FA-MS) was evaluated as a protection method on also other artificially patinated bronzes. Brown patina was achieved by applying Cu_2S over bronze, while a green patina was deliberately developed to resemble a less stable sulphate-based corrosion product, found on bronze sculptures exposed outdoors [9]. Additionally, since the 3-mercapto-propyl-trimethoxysilane show interesting alternative for the brown patina protection [13], a new, tailored fluoropolymer coating with the addition of mercaptopropyl groups (abbreviated in the scope of this paper as FA-MS-SH) was developed and evaluated on one brown and two green sulphate patinas, as well as on bare bronze.

Multiple electrochemical techniques were used to study the corrosion properties, including measurement of corrosion potential and potentiodynamic scans. SEM, optical microscopy, Raman and XRD analysis were employed to analyze the corrosion products formed on samples exposed to artificial urban rain.

2. Material and methods

2.1. Bronze samples, patination and preparation of the coatings

2.1.1. Bronze and patination

The chemical composition, in wt%, of the tested bronze was 6.9 Sn, 3.1 Zn, 2.0 Pb and Cu in balance. This composition is typical of a quaternary as-cast bronze used in an art foundry [1]. Bronze samples were cut into 5 cm × 2.5 cm bronze plates and chemically etched in order to remove all the dirt and previous oxides. All samples were then abraded with 1200 grit SiC paper and ultrasonically cleaned for 3 min in acetone.

Three artificially prepared patinas were studied, as well as the corresponding bare bronze. The artificially prepared patinas tested were: (a) a brown patina, (b) a sulphate-type patina applied over the brown patina, and (c) a persulphate patina applied over the brown patina. The brown patina applied on the bronze was achieved by preheating the surface then brushing it with a 3% K_2S solution (all % in this paper are given in weight percent). The surface was then rinsed under running tap water. The sulphate and persulphate patinas were each applied over the brown patina. The green sulphate patina was applied over the brown patina by brushing it with a solution of 30% $(NH_4)_2SO_4$, 0.95% $CuSO_4{\cdot}5H_2O$ and 0.16% NH_3. The sulphate patina was developed in the presence of high humidity. The green persulphate patina was achieved by applying a solution of 25.9% $(NH_4)_2S_2O_8$, 0.95% $CuSO_4{\cdot}5H_2O$ and 1.22% of NH_3 to the sample. All chemicals were of p.a. quality. In order to get a well-defined green colour the brown patina was left to stand for 24 h. The various patinas are presented in Fig. 1. The reference surface, patinated surfaces, and protected surfaces were then electrochemically tested in order to study their electrochemical properties.

2.1.2. Preparation of the coatings

Methyl methacrylate was provided by Akripol and 3-ethacryloxypropyltrimethoxysilane was obtained from ABCR GmbH&Co. Funcosil AG, a commercial product from Remmers, was used as the source of fluoroacrylate. Lauroyl peroxide, (3-mercaptopropyl) trimethoxysilane, diethyl succinate, n-butyl acetate and n-heptane were obtained from Sigma Aldrich.

The way in which the syntheses were carried out has been described in detail elsewhere [7]. Briefly, the adhesion promoter methyl methacrylate and methacryloxypropyl-trimethoxysilane (abbreviated as MS) were synthesized by the copolymerization of methyl methacrylate and methacryloxypropyl-trimethoxysilane (9:1 molar ratio) in acetone with 2% lauroyl peroxide used as an initiator. The reaction temperature was 55 °C, and the reaction time 72 h. After the reaction was completed, the solvent exchange was performed as follows, the diethyl succinate was added to the reaction vessel, and acetone was evaporated at a reduced pressure at room temperature to form a 20% solution. Dry fluoropolymer was obtained by drying a commercial solution of fluoroacrylate polymer at 60 °C for several days.

The fluoropolymer coating (FA-MS) was composed of 10% MS and 5% fluoroacrylate polymer dissolved in a mixture of solvent (diethyl succinate and n-butyl acetate in a 3:2 mass ratio).

An alternative fluoropolymer protective coating (FA-MS-SH) was also developed, which was composed of two solutions: (1) 10% MS and 0.5% (3-mercaptopropyl)trimethoxysilane solution in diethyl succinate and n-butyl acetate in a 3:2 mass ratio, and (2) 5% fluoroacrylate polymer in n-heptane.

2.1.3. Application of the protective coatings and curing

The FA-MS coating was applied by self-assembled single layer technique as already described in our previous paper [7] using brush using a coverage rate of around 2.4–3 g/m^2. The coated samples were dried and cured at 40 °C in an oven for at least 24 h.

The FA-MS-SH coating was applied by layer by layer technique (in two layers) using a brush. The first layer was applied using a coverage rate of around 1.6 g/m^2. The coated samples were then dried and cured at 40 °C in an oven for 2 h, before applying the second layer using 0.8 g/m^2 coverage rate. The coated samples were then dried and cured at 40 °C in an oven for 24 h.

2.2. Surface investigation techniques

2.2.1. XRD analysis

The phase analysis of the samples was performed by X-ray diffraction (XRD), using an Empyrean diffractometer (PANalytical, Netherlands) with Cu–Kα radiation. Powder diffraction data was collected at room temperature, at a tube tension of 45 kV and a tube current of 40 mA, using a 2θ step size of 0.013° and a measurement time of 150 s per step. Data was collected over a 2θ range of 10° to 70°. The results were analyzed by Highscore (PANalytical, Netherlands) diffraction software.

XRD analyses were carried out on powders of the scraped green patinas that were initially chemically applied. Same amount of material was used for analysis.

The results of the XRD analysis were analyzed by Highscore

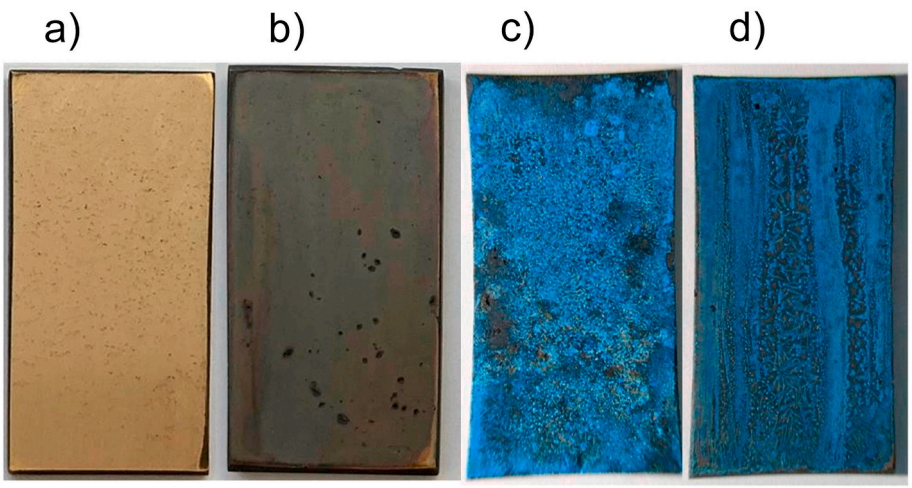

Fig. 1. Photographic images of the bare bronze (a) and the different patinas: brown patina (b), sulphate patina on brown patina (c) and persulphate patina on brown patina (d). (For interpretation of the references to colour in this figure legend, the reader is referred to the web version of this article.)

(PANalytical, Netherlands) diffraction software (version 4.8), using the Powder Diffraction File PDF-4+ (2020, ICDD, USA) database as a source of reference data. The following powder diffraction file numbers were used: brochantite PDF# 04-011-4170; prosnjakite PDF# 04-010-7185; antlerite PDF# 01-072-6504.

2.2.2. Raman microscopy

Raman analysis of the patina samples was performed using a 532 nm laser excitation line with a Bruker's SENTERA II dispersive Raman micro-spectrometer. The spectra were recorded using a ×100 objective lens and a 400 grooves/mm grating, which gave a spectral resolution of approx. 4 cm^{-1}. The power at the samples was set to 2.5 mW using neutral density filters. A multi-channel, TE (thermo-electrically) cooled CCD detector was used, with the integration time set to 15 s, and the spectral range between 50 and 4200 cm^{-1}. Wave number calibration was performed using a styrene reference sample. The Raman spectra presented in the paper are stated without baseline correction.

2.2.3. Measurement of colour variation

The variation in colour of each sample was evaluated using the same method as has been described in detail elsewhere [7]. Briefly, the *Lab* values (CIE 1976 $L^*a^*b^*$ or CIELAB colour space) were measured at four different areas on each sample, before and after application of the coating, using an i1 colourimeter (X-Rite). The system operates using a 45/0 measuring geometry, a D65 illuminant and a 5-mm sample aperture. In order to analyze the same area of the bronze samples both before and after application of the coating, a jig with four defined measuring areas was used. The total colour difference, ΔE^*, was calculated using Eq. (1) (the uncoated surface was used as reference for calculation ΔE^*). Throughout the manuscript results are presented as the average values of these four *Lab* values, along with standard deviations.

$$\Delta E^* = \left(\Delta L^{*2} + \Delta a^{*2} + \Delta b^{*2}\right)^{1/2} \quad (1)$$

2.3. Electrochemical testing

Electrochemical tests were conducted using Gamry Frameworks on a Gamry Reference 600 potentiostat/galvanostat. All experiments were conducted in a standard three-electrode cell, using a saturated calomel reference electrode (SCE), a graphite counter electrode, and a working electrode made of either bare or patinated bronze with an exposed surface area of 3.3 cm^2. All potentials in the text refer to potential vs the SCE scale. Electrochemical testing of the bronze, patinas and coatings was conducted in a simulated acid rain solution at a pH of 3.3 and conductivity of 345 μS/cm at 25 °C. The simulated urban rain solution contained 14.4 mg/L $CaSO_4$ $2H_2O$, 15.0 mg/L $(NH_4)_2SO_4$, 19.1 mg/L NH_4Cl, 15.1 mg/L $NaNO_3$, 39.3 μL/L HNO_3 (65 wt%), 31.9 mg/L CH_3COONa and 8.0 mg/L HCOONa [17].

At first, open circuit potential was measured for at least 1 h or until stable potential was reached. Then linear polarization measurements were executed in potential range ± 20 mV vs E_{corr} at a scan rate of 0.1 mV/s. Then, dynamic potential scan was executed starting −250 mV vs E_{corr} and progressing anodically up to 1 V vs E_{ref} with a scan rate of 0.167 mV/s. E_{corr}-corrosion potential and j_{corr}-corrosion current density were extracted from electrochemical measurements.

Protection efficiency η was calculated using Eq. (2):

$$\eta\% = [1 - (j_{corr}'/j_{corr})] \times 100 \quad (2)$$

where j_{corr}' is protected and j_{corr} is unprotected corrosion current density.

2.4. Microscopic analysis and contact angle measurements

The morphology of the different patinas was observed via scanning electron microscopy (SEM), using a Jeol JSM IT500 LV scanning electron microscope (Joel, Tokyo, Japan, 2019). SEM observations took place in a high vacuum at an accelerating voltage of 20 kV. EDS analyses were performed using a Link Pentafet (Oxford Instruments, London, UK, 2019).

Contact angle measurements were performed by means of the static method, using the FTA 1000 DropShape Instrument B FrameSystem (First Ten Angstroms, Newark, USA). A droplet of distilled water (2 μL) was placed on the bronze surface and an image recorded. The static contact angle was defined by fitting the Young–Laplace equation. Measurements were performed in at least three different areas, with the average values being expressed as the result.

3. Results and discussion

3.1. Patina analysis

The surfaces of the bare bronze and various patinated surfaces, namely a brown patina, a sulphate patina and a persulphate patina, were examined using SEM. The images of the surfaces are presented in Fig. 2 at equal magnifications, while the elemental compositions obtained from EDS analysis are presented in Table 1.

In Fig. 2a, the surface grinding marks are visible on the bronze; EDS analysis showed the elemental composition of the bronze, with some

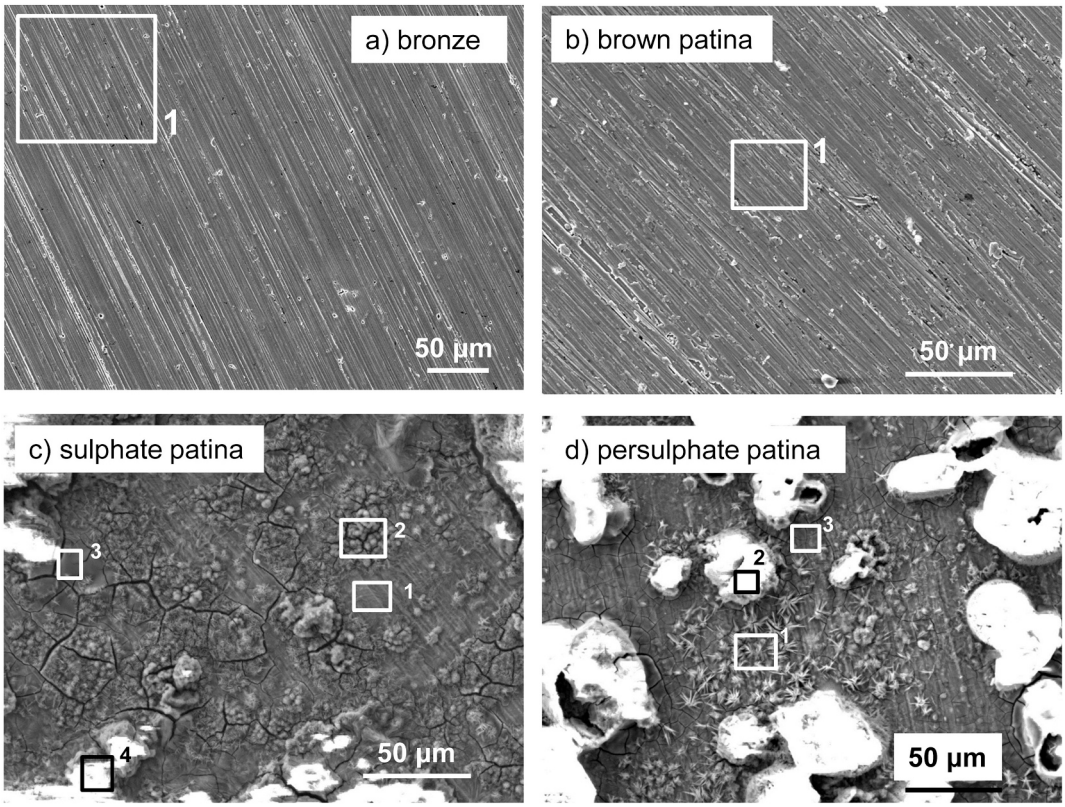

Fig. 2. SEM images of the bronze (a) and the various patinas: brown patina (b), sulphate patina on brown patina (c) and persulphate patina on brown patina (d).

Table 1
EDS analysis of the bronze and bronzes patinated with brown, sulphate and persulphate patinas, in wt%.

	Cu	Sn	Zn	Pb	C	O	S	K	Al	Fe	Si	Cl
Bronze	87	7.38	3.30	1.47		0.9						
Brown patina (1)	73.1	5.4	3.2	0.7	8.5	4.3	4.0	0.1	0.2	0.2	0.1	/
Brown patina (2)	67.2	4.8	3.1	/	12.7	4.8	7.1	0.1	0.3	/	/	/
Sulphate patina (1)	58.8	1.5	1.5	/	6.5	22.3	9.1	0.2	/	/	/	/
Sulphate patina (2)	47.7	0.5	5.0	/	7.8	32.5	6.6	/	/	/	/	/
Sulphate patina (3)	37.0	/	3.0	/	10.4	43.5	6.0	/	/	/	/	/
Sulphate patina (4)	48.1	/	3.6	/	7.5	33.9	6.9	/	/	/	/	/
Persulphate patina (1)	44.3	2.7	6.4	2.0	7.1	30.9	6.7	/	/	/	/	/
Persulphate patina (2)	42.1	/	3.9	/	10.3	37.2	6.4	/	/	/	/	0.2
Persulphate patina (3)	56.4	2.9	2.0	/	7.1	23.5	8.1	/	/	/	/	/
	Cu	Sn	Zn	Pb	C	O	S	K	Al	Fe	Si	Cl

oxygen and carbon present at the surface. In Fig. 2b, the SEM image of the brown patinated surface is shown. EDS analysis showed the presence of sulphur, oxygen and carbon, next to the alloying elements of bronze. Flakes of a thicker layer of Cu_2S are present in small patches, as is also visible from the higher sulphur content (not marked on the image, EDS composition (2) shown in Table 1). Fig. 2c presents the surface morphology of the sulphate patina that formed over the brown patina. Four distinctive regions are observed and analyzed. In area 1, the flat surface still reveals the grinding marks, and EDS analysis showed that S and O are still present in high quantities. In area 2, there is an agglomerate of round crystals. A larger quantity of O and Zn is found compared to area 1, while area 3 is richer in the elements C and O. At higher (not shown) magnifications it can be seen that the layers that developed are thicker in areas 2 and 4; they are flat, and cracked, with tiny needle like crystals. A similar composition was measured in both areas (Table 1). Fig. 2d reveals the surface morphology of the persulphate patina that formed over the brown surface. The fine needle type crystals are present in area 1 in a flower like structure. Carbon, oxygen and sulphur were found, along with elements from the bronze. In area 2, a big agglomerate of corrosion products is present, with a similar composition to that of area 1; only Sn and Pb were not detected. Area 3 is flatter, with visible grinding marks in the area where a greater amount of sulphur was detected. Probably, in these areas, the brown patina prevails.

3.1.1. *Raman analysis*

Raman shifts at 282, 328 and 615 cm^{-1} (Fig. 3a) indicate the presence of Cu_2S [18]. Both sulphate-based patinas show the strongest band at 975 cm^{-1} (Fig. 3b and c), which signifies the stretching vibration of SO_4^{-2} [19,20]. Two well defined bands at 3587 and 3565 cm^{-1}, in the OH^- stretching region, as well as Raman shifts at 3400 and 3262 cm^{-1} (Fig. 3b), indicate the presence of brochantite ($Cu_4(OH)_6SO_4$), which is also confirmed by the peaks in the lower wavenumber region at 1128, 1101, 1075, 910, 607, 507, 480, 449, 389, 244, and 143 cm^{-1} [19,20]. In the persulphate patina (Fig. 3c) the bands in the OH^- stretching region are far less defined, appearing as a broadened band with several maxima at 3556, 3408 and 3269 cm^{-1}. This, along with the Raman shifts in the lower wavenumber region at 1151, 1118, 1068, 612, 504, 447,

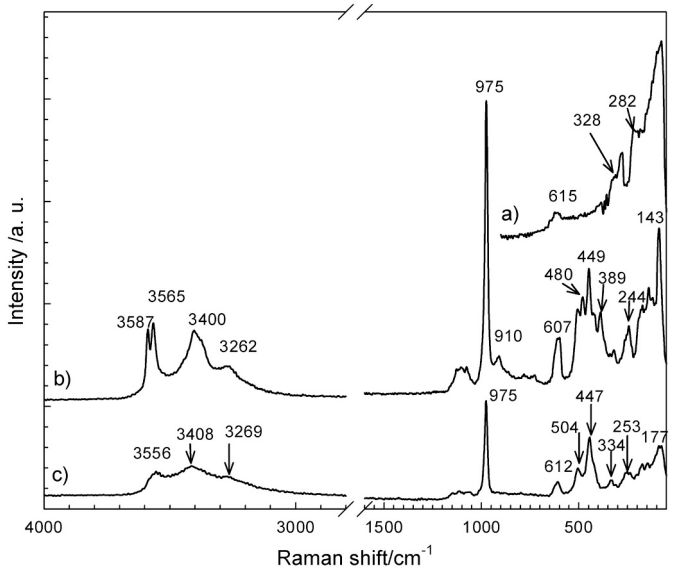

Fig. 3. Raman analysis of the (a) brown (b) sulphate and (c) persulphate patinas.

334, 253, and 177 cm^{-1}, suggest that posnjakite ($(Cu_4(OH)_6SO_4)\cdot H_2O$) was the primary constituent [19,20].

3.1.2. XRD analysis

Further analyses were performed in order to find possible differences between the sulphate and persulphate patinas over the whole surface of the patinated bronzes. The same amount of patina was analyzed on the sulphate and persulphate patinated samples in order to estimate the quantitative presence of certain mineral phases.

The XRD pattern of the sulphate (SP) and persulphate (PSP) patinas are presented in Fig. 4. The presence of mineral phases is denoted, with B representing brochantite, P, posnjakite, and A, antlerite. In both samples the mineral phase posnjakite ($Cu_4SO_4(OH)_6\cdot H_2O$) predominates. Brochantite ($Cu_4SO_4\cdot(OH)_6$) and antlerite ($Cu_3(SO_4)(OH)_4$) are also present in smaller amounts.

Given that the same amount of material was used for analysis (and the fact that both samples were prepared in the same way – the patinas were scraped from the surfaces of the samples and the powder was analyzed), in relative comparison the amount of brochantite is slightly higher in the SP sample, with the distinguishable peaks denoted by arrows in Fig. 4. The intense lines found at 12°, 13.8°, 22.6°, 36° and 53° in the pattern of both patinas are characteristic of brochantite. The distinguishable lines at 18.3° (a peak which does not overlap with any of the other phases (2 Θ at 18.3°)), 23.7°, 34°, 36.5° and 42° suggest the presence of antlerite. Based on this data it can be concluded that the minerals posnjakite and brochantite were probably formed by preparing the green sulphate-based patina, whereas in the sulphate patina (SP) the amount of brochantite is higher and antlerite is present in trace amounts.

3.2. Hydrophobicity and colour change following application of the coating

Average values for the contact angle measurements of the samples' surfaces are given in Table 2. The contact angles on the unprotected patinas are low (37–49°); it is higher (86°) in the unprotected bare bronze, which was ground with 1200 grit SiC paper. Where the FA-MS coating was applied to the bare and patinated surfaces, the contact angle is higher, with values between 112° and 120°. The FA-MS-SH

Table 2
Contact angles of the bronze, brown patina, sulphate patina and persulphate patina when unprotected and following the application of two different types of protective coating (average values with standard deviations).

Type of patina/ coating	Unpatinated bronze	Brown patination	Sulphate patination	Persulphate patination
Unprotected [°]	86 ± 5	37 ± 11	39 ± 6	49 ± 8
Fluoropolymer coating (FA-MS) [°]	116 ± 0.3	112 ± 0.5	119 ± 0.6	120 ± 1.0
Alternative fluoropolymer coating (FA-MS-SH) [°]	116 ± 0.7	115 ± 0.9	128 ± 2.6	126 ± 3.5

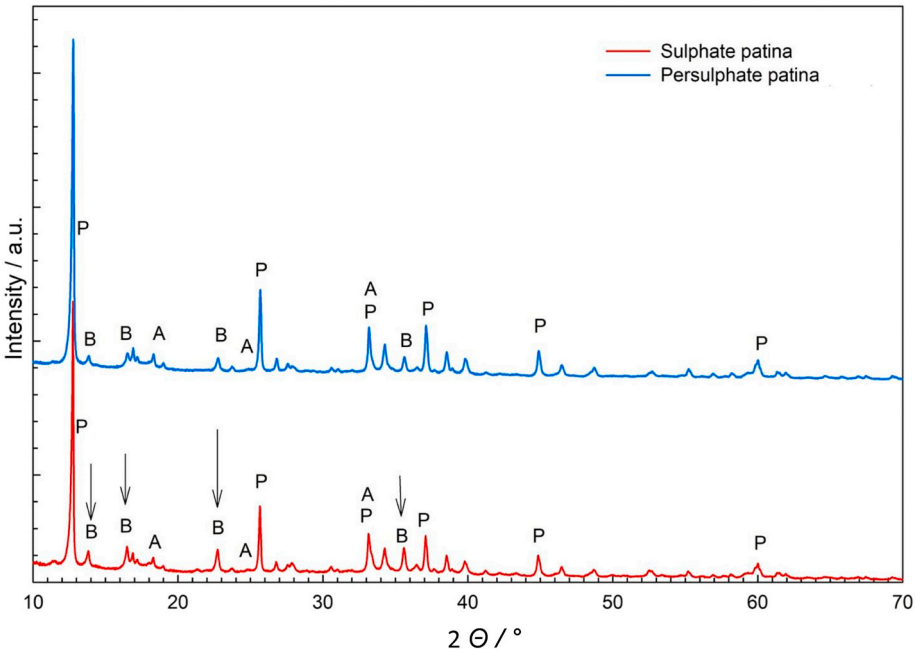

Fig. 4. XRD patterns of the sulphate and persulphate patinas.

protection resulted in even higher contact angles, especially for the samples with sulphate and persulphate patinas (128° and 126°, respectively) (Fig. 5).

The colour variations in samples following the application of different coatings were evaluated by colour differences (ΔE^*), which are presented in Table 3. The application of either FA-MS or FA-MS-SH coatings on the unpatinated bronze and brown patinated samples resulted in ΔE^* values between 8 and 13 (see Table 3, first and second columns), whereas the application of FA-MS or FA-MS-SH coatings on the sulphate or persulphate patina resulted in smaller changes in ΔE^* (ΔE^* of 2 or 3, see third and fourth columns in Table 3). According to a report by Mokritzky et al., the standard observer sees colour differences as follows: ΔE values between 2 and 3.5 correspond to the difference could be noticed by unexperienced observer, whereas when ΔE values are higher than 5, the observer would notice two different colours [21]. Taking this into account, it can be concluded that the application of coatings affects the change in colour in all samples, but that this change is less pronounced in samples with the sulphate and persulphate patinas.

3.3. Electrochemical evaluation of patina coatings

The results of potentiodynamic measurements for the bare and patinated bronzes, with and without the two different types of protective coating, are presented in Figs. 6, 7, 8 and 9. Corrosion current density, j_{corr}, and corrosion potential, E_{corr}, were deduced from the polarization curves and are presented in Table 4.

The E_{corr} for bare bronze in simulated urban rain was −0.156 V (Fig. 6, Table 4). The corrosion current density was 0.948 μA/cm^2. Both cathodic and anodic current density decreased when a FA-MS was applied to the bronze, and j_{corr} reduced to 0.0126 μA/cm^2. When the FA-MS-SH coating was applied, j_{corr} decreased to a value of 0.358 μA/cm^2. Protection efficiency for the FA-MS and FA-MS-SH coatings was 99% and 62%, respectively.

The E_{corr} value for the brown patinated bronze (−0.198 V) is more negative than that of the bare bronze (Fig. 7, Table 4). In the brown patina j_{corr} is higher than in the bare bronze, as would be expected given that a sulphide patina is more reactive in simulated urban rain. Following the application of the FA-MS coating, a decrease was observed in the anodic current density in the anodic part of the potentiodynamic curve, while only a moderate decrease in j_{corr} of 1.75 μA/cm^2, occurred. The application of the FA-MS-SH coating over the brown patina resulted in a reduced j_{corr}, and more positive E_{corr} value. The alternative fluoropolymer protection FA-MS-SH method was more effective on brown patina than on the bare bronze, as can be observed from the electrochemical experiments.

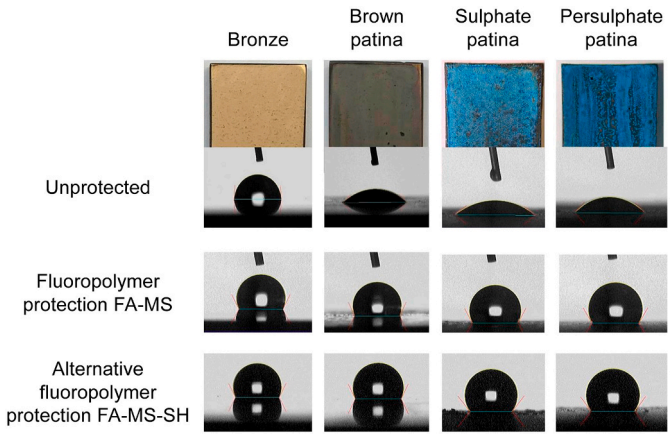

Fig. 5. Contact angles of the bare and patinated bronze, unprotected and then following the application of two different types of fluoropolymer protective coating (FA-MS and FA-MS-SH).

Table 3
Colour variations.

Type of patina	Unpatinated bronze Colour variation ΔE*	Brown patination Colour variation ΔE*	Sulphate patination Colour variation ΔE*	Persulphate patination Colour variation ΔE*
Fluoropolymer coating FA-MS	13 ± 1	8 ± 1	2 ± 0	3 ± 0.5
Alternative fluoropolymer coating (FA-MS-SH)	11 ± 1	9 ± 3	2.0 ± 0.5	3.0 ± 0.5

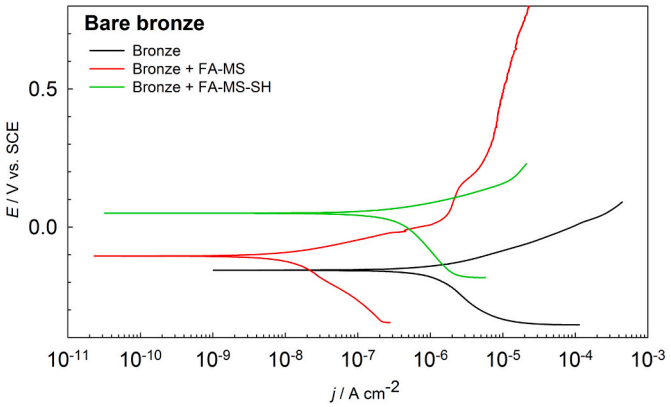

Fig. 6. Polarization curves for bare bronze with different types of protection: black curve – unprotected bronze, red curve – fluoropolymer coating FA-MS, green curve – alternative fluoropolymer protective coating FA-MS-SH. Scan rate = 0.167 mV/s. (For interpretation of the references to colour in this figure legend, the reader is referred to the web version of this article.)

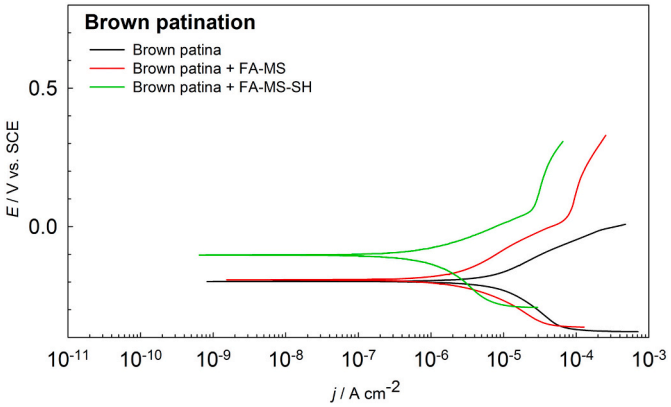

Fig. 7. Polarization curves for brown patinated bronze with different types of protection: black curve – unprotected bronze, red curve – fluoropolymer coating FA-MS, green curve – alternative fluoropolymer protective coating FA-MS-SH. Scan rate = 0.167 mV/s. (For interpretation of the references to colour in this figure legend, the reader is referred to the web version of this article.)

In the sulphate patinated bronze j_{corr} was as high as 30.2 μA/cm^2, and E_{corr} −0.081 V (Fig. 8, Table 4). The activity of such patination over bronze is the highest.

When the FA-MS coating was applied, the current densities in the cathodic and anodic regions decreased. With the FA-MS coating j_{corr} was 5.64 μA/cm^2, resulting in a protection efficiency of 82%. Using the alternative fluoropolymer protection FA-MS-SH on the sulphate patinated bronze resulted in a further decrease in j_{corr}, to 2.01 μA/cm^2. With a protection efficiency of 93%, the FA-MS-SH coating offered better

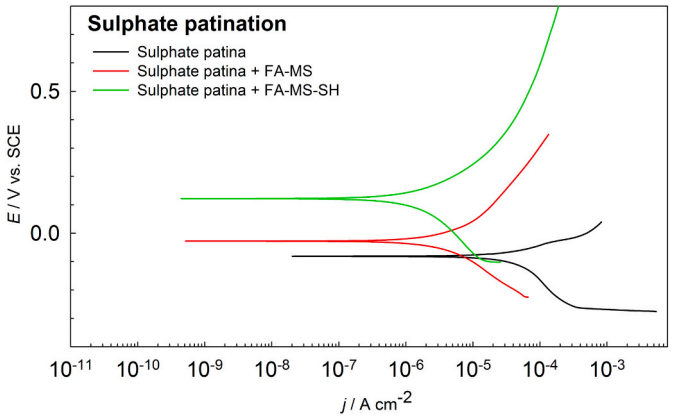

Fig. 8. Polarization curves for green sulphate patinated bronze with different types of protection: black curve – unprotected bronze, red curve – fluoropolymer FA-MS coating, green curve – alternative protective fluoropolymer coating FA-MS-SH. Scan rate = 0.167 mV/s. (For interpretation of the references to colour in this figure legend, the reader is referred to the web version of this article.)

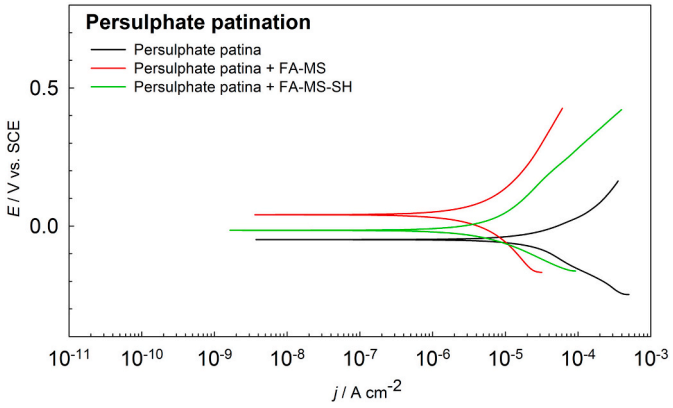

Fig. 9. Polarization curves for green persulphate patinated bronze with different types of protection: black curve – unprotected bronze, red curve – fluoropolymer coating FA-MS, green curve – alternative protective fluoropolymer coating FA-MS-SH. Scan rate 0.167 mV/s. (For interpretation of the references to colour in this figure legend, the reader is referred to the web version of this article.)

Table 4
Electrochemical parameters, E_{corr}, j_{corr} and protection efficiency for the various substrates and protective methods.

Sample/coating	E_{corr} (V)	j_{corr} (μA/cm^2)	Protection efficiency %
bronze	−0.156	0.948	
Bronze + FA-MS	−0.105	0.0126	98.6
Bronze + FA-MS-SH	−0.0378	0.358	62.2
Brown patina	−0.198	4.09	
Brown patina + FA-MS	−0.192	1.75	57.2
Brown patina + FA-MS-SH	−0.102	0.90	78.0
Sulphate patina	−0.0814	30.9	
Sulphate patina + FA-MS	−0.0279	5.64	81.7
Sulphate patina + FA-MS-SH	0.0339	2.01	93.5
Persulphate patina	−0.049	18.1	
Persulphate patina + FA-MS	0.08	4.00	77.9
Persulphate patina + FA-MS-SH	−0.015	6.21	65.7

protection than the fluoropolymer coating FA-MS in this case.

When the persulphate patina was applied over the brown patina, the j_{corr} is smaller than in the case of the sulphide patina, but, at 18.1 μA/cm^2, still relatively large (Fig. 9, Table 4).

When comparing electrochemical properties of bronze, brown and sulphate type of patinas, it can be seen that E_{corr} values for sulphate type patinas are slightly more positive. Also, cathodic current densities in potentiodynamic curves are higher when compared to bronze in simulated rain, as a result also j_{corr} values for sulphate type of patinas are higher in comparison to that of bronze (see Table 4).

Using the fluoropolymer FA-MS coating over the persulphate patina led to a reduction in the current densities of the cathodic and anodic processes, resulting in a j_{corr} of 4 μA/cm^2, and a protection efficiency of 78%. The alternative fluoropolymer protective coating FA-MS-SH resulted in a j_{corr} of 6.21 μA/cm^2, and 66% protection efficiency.

3.4. Mechanism of protection

The contact angles are similar across most of the samples, with slightly higher values seen in the sulphate and persulphate patinated samples with the FA-MS-SH coating. This could be the result of the increased roughness of these samples, in addition to the layered application of the AP coating, which ensures the strict presence of a fluoropolymer layer on the uppermost surface. The sulphate and persulphate patina show mainly similar composition - according to XRD patterns prosnjakite $Cu_4SO_4(OH)_6{\cdot}H_2O$ dominates in both patinas, while the amount of brochantite $Cu_4SO_4{\cdot}(OH)_6$ was slightly higher in sulphate patina layer, proved also with more clearly defined shifts for the OH stretching region in Raman spectra.

Schematic representations of a potential mechanism for the bonding of molecules to the patinated surfaces are given in Figs. 10 and 11 for the FA-MS and FA-MS-SH coatings, respectively.

We proposed following explanation for FA-MS coating (see Fig. 10): the bare bronze substrate forms in air atmosphere a very thin layer of oxide, which has good affinity with the silanol groups of the silane-modified poly methylmethacrylate (MS), possibly forming covalent and hydrogen bonds, resulting in a high protection efficiency (98%, Fig. 10).

On the brown patina, which has a layer of copper sulphide (see Raman spectra), the affinity to silanol groups of MS of FA-MS coating is proposed to be lower, yielding a lower protection efficiency for FA-MS coating (58%, Fig. 10).

Sulphate and persulphate patinas result in similar protection efficiency, 81 and 78%, respectively, probably correlated with similar structural composition of patinas.

The alternative fluoropolymer protection FA-MS-SH coating contains silane-modified poly methylmethacrylate (MS) with added mercaptopropyltrimethoxy silane (SH) and a fluoroacrylate layer (FA). We proposed following explanation for FA-MS-SH coating: the mercapto group of 3-mercaptopropyltrimethoxysilane (SH) has affinity to attach to sulphide rich areas of brown patina, whereas silanols groups mainly form connections with MS molecules (see Fig. 11).

Namely, on the brown patina, which has a layer of copper sulphide, the protection efficiency was much higher in the case when FA-MS-SH coating was applied when compared to FA-MS applied over brown patina (78% vs 57%, respectively, see results in Figs. 10 and 11, right inset scheme and values for brown patina). This agrees well with reports in literature, where 3-mercapto-propyl-trimethoxysilane coating (PropS-SH) was found to be highly efficient on brown patinated surfaces [13]. On bare bronze, however, the protection efficiency of the FA-MS-SH coating is much lower than that of the FA-MS coating (62% vs 99%, respectively, see results in Figs. 10 and 11, left inset scheme and values are for bare bronze), therefore strong C-S-Cu bonds were not proposed. The hypothesis has to be proved in future studies.

On the sulphate patina, the protection efficiency of the FA-MS-SH increased to 94% and is even higher as in the case of FA-MS-SH

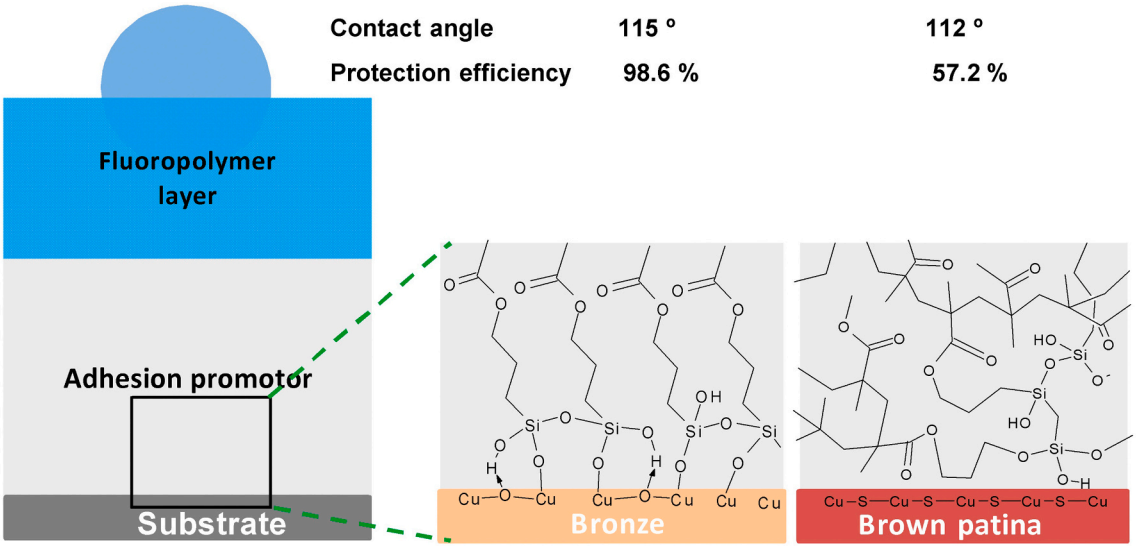

Fig. 10. Schematic representation of the potential protection mechanism of the FA-MS coating on bare bronze and brown patinated bronze substrates.

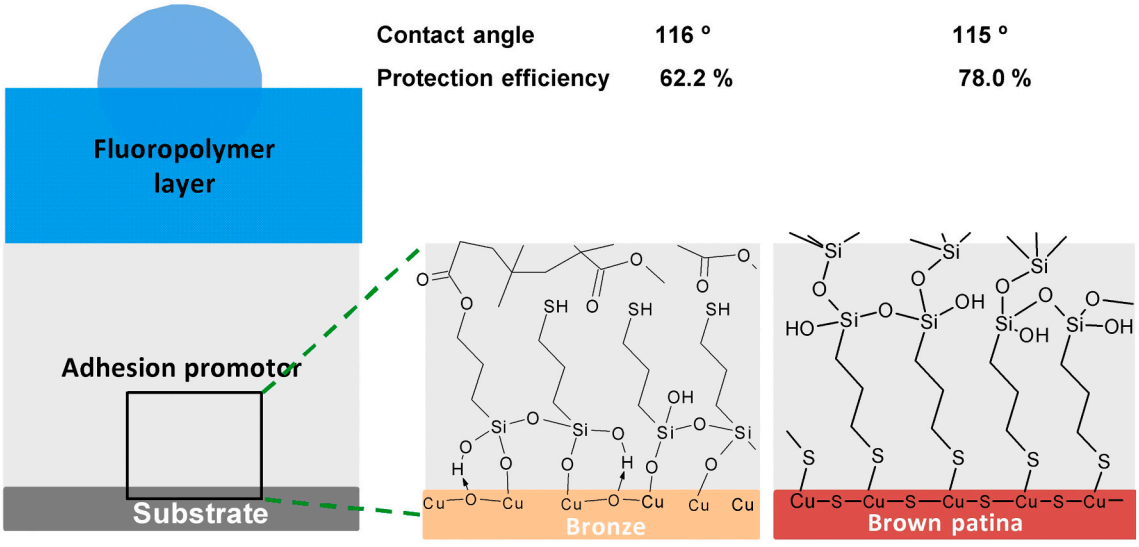

Fig. 11. Schematic representation of a possible mechanism of protection for the FA-MS-SH coating on bare bronze and brown patinated substrate.

applied on the brown patina (Cu_2S layer) or on the bare bronze with thin oxide layer. The protection efficiency of persulphate patina, which shows similar structural composition (see XRD pattern), is somewhat lower (66%). The possible difference in protection efficiency is the surface coverage difference, which might be different on persulphate type of patina, which was more voluminous and thicker, thus inhomogenous. The proof of this difference is beyond the scope of this work, and requires more detailed investigation in future studies.

4. Conclusions

Two different fluoropolymer based protection systems were tested in order to find the optimal protection of bare and differently patinated bronze surfaces for application in an outdoor environment. The following conclusions were made.

- Raman analysis revealed that the brown patina consisted primarily of Cu_2S, while the sulphate and persulphate green patinas consisted of posnjakite and brochantite, with the brochantite predominantly found on the sulphate type patina, as confirmed by XRD analysis.
- Two types of protection coatings were developed and tested. The first was a fluoropolymer coating with silane-modified poly methylmethacrylate (MS) (FA-MS coating), which was applied in one layer. The second coating was an alternative fluoropolymer protective coating (FA-MS) with added mercaptopropyltrimethoxy silane (SH) and applied layer-by layer (FA-MS-SH coating).
- After protecting samples with one of each fluoropolymers coatings, the change in colour was smaller in the samples with sulphate-type patinas compared to that in the bare bronze and brown patinated samples.
- Electrochemical testing was conducted to evaluate the protection efficiency. The corrosion study in simulated rain showed that bare bronze was protected most efficiently by the fluoropolymer coating - FA-MS (99%). In the brown patinated samples, the newly developed alternative fluoropolymer coating - FA-MS-SH (78%) offered the most efficient protection. The sulphate patina, which contains mainly posnjakite and some brochantite, was protected by the alternative coating - FA-MS-SH with 94% efficiency, while the persulphate patina, which primarily consists of posnjakite, was well

protected by the fluoropolymer coating - FA-MS, with 78% protection efficiency.
- Mechanisms of protection were suggested for the different types of patina. It is proposed that the protection efficiency varies due to the differences of affinity of constituent components of studied coatings.

CRediT authorship contribution statement

T. Kosec: Conceptualization, Investigation, Writing - Original draft preparation, Reviewing and editing, Supervision, **Ž. Novak:** Investigation, Formal analysis, **E. Švara-Fabjan:** Validation, Writing - Review & editing, **L. Škrlep:** Investigation, Writing - Review & editing, **A. Sever-Škapin:** Supervision, Writing - Review & editing, **P. Ropret:** Investigation, Funding acquisition, Writing - Review & editing.

Declaration of competing interest

The authors declare that they have no known competing financial interests or personal relationships that could have appeared to influence the work reported in this paper.

Acknowledgment

The financial support received from the Slovenian Research Agency (SRA) for project no J7-9404 and program P2-0273 is hereby gratefully acknowledged. Thanks to Nina Gartner for performing SEM/EDS analysis and Vesna Zalar Serjun for the analysis and discussion of XRD results.

References

[1] P. A. Schweitzer, Fundamentals of metallic corrosion: atmospheric and media corrosion of metals, Corrosion Engineering Handbook, 2nd ed., CRC press, Taylor&Francis Group, NY 2007. doi:https://doi.org/10.1021/ja076915w.
[2] V.N. Naudé, Guide to the Maintenance of Outdoor Sculpture, American Institute for Conservation of Historic and Artistic Works, Washington, D.C, 1993.
[3] E. Franceschi, P. Letardi, G. Luciano, Colour measurements on patinas and coating system for outdoor bronze monuments, J. Cult. Herit. 7 (2006) 166–170, https://doi.org/10.1016/j.culher.2006.03.001.
[4] E. Cano, D. La Fuente, D.M. Bastidas, Use of EIS for the evaluation of the protective properties of coatings for metallic cultural heritage: a review, J. Solid State Electrochem. 14 (2010) 381–391, https://doi.org/10.1007/s10008-009-0902-6.
[5] G. Bierwagen, T.J. Shedlosky, K. Stanek, Developing and testing a new generation of protective coatings for outdoor bronze sculpture, Prog. Org. Coat. 48 (2003) 289–296, https://doi.org/10.1016/j.porgcoat.2003.07.004.
[6] M. Mihelčič, L. Slemenik Perše, E. Šest, I. Jerman, C. Giuliani, G. Di Carlo, M. Lavorgnac, A.K. Surca, Development of solvent- and water-borne fluoropolymer protective coatings for patina-free bronze discs, Prog. Org. Coat. 125 (2018) 266–278, https://doi.org/10.1016/j.porgcoat.2018.09.014.
[7] T. Kosec, L. Škrlep, E. Švara Fabjan, A. Sever Škapin, G. Masi, E. Bernardi, C. Chiavari, C. Josse, J. Esvan, L. Robbiola, Development of multi-component fluoropolymer based coating on simulated outdoor patina on quaternary bronze, Prog. Org. Coat. 131 (2019) 27–35, https://doi.org/10.1016/j.porgcoat.2019.01.040.
[8] P. Piccardo, V. Bongiorno, S. Campodonico, Artistic patinas on ancient bronze statues, in: Corrosion and Conservation of Cultural Heritage Metallic Artefacts, European Federation of Corrosion (EFC) Series, 2013, pp. 193–212, https://doi.org/10.1533/9781782421573.3.193.
[9] G. Di Carlo, C. Giuliani, C. Riccucci, M. Pascucci, E. Messina, G. Fierro, M. Lavorgna, G.M. Ingo, Artificial patina formation onto copper-based alloys: chloride and sulphate induced corrosion processes, Appl. Surf. Sci. 421 (2017) 120–127, https://doi.org/10.1016/j.apsusc.2017.01.080.
[10] L. Muresan, S. Varvara, E. Stupnišek-Lisac, H.Otmačić Ćurković, K. Marušić, S. Horvat-Kurbegović, L. Robbiola, K. Rahmouni, H. Takenouti, Protection of bronze covered with patina by innoxious organic substances, Electrochim. Acta 52 (2007) 7770–7779, https://doi.org/10.1016/j.electacta.2007.02.024.
[11] R. Bostan, S. Varvara, L. Gaina, T. Petrisor Jr., L.M. Muresan, Protective effect of inhibitor-containing nitrocellulose lacquer on artificially patinated bronze, Prog. Org. Coat. 111 (2017) 416–427, https://doi.org/10.1016/j.porgcoat.2016.08.004.
[12] E. Apchain, D. Neff, J.-P. Gallien, N. Nuns, P. Berger, A. Noumowé, P. Dillmann, Efficiency and durability of protective treatments on cultural heritage copper corrosion layers, Corros. Sci. 183 (2021), https://doi.org/10.1016/j.corsci.2021.109319.
[13] G. Masi, J. Esvan, C. Chiavari, E. Bernardi, C. Martini, M.C. Bignozzi, C. Monticelli, F. Zanotto, A. Balbo, E. Svara Fabjan, T. Kosec, L. Robbiola, Evaluation of the protectiveness of an organosilane coating on patinated Cu-Si-Mn bronze for contemporary art, Prog. Org. Coat. 127 (2019) 286–299, https://doi.org/10.1016/j.porgcoat.2018.11.027.
[14] T. Kosec, H. Otmačić Ćurković, A. Legat, Investigation of the corrosion protection of chemically and electrochemically formed patinas on recent bronze, Electrochim. Acta 56 (2010) 722–731, https://doi.org/10.1016/j.electacta.2010.09.093.
[15] H. Otmačić Ćurković, T. Kosec, K. Marušić, A. Legat, An electrochemical impedance study of the corrosion protection of artificially formed patinas on recent bronze, Electrochim. Acta 83 (2012) 28–39, https://doi.org/10.1016/j.electacta.2012.07.094.
[16] T. Wang, J. Wang, Y. Wu, The inhibition effect and mechanism of l-cysteine on the corrosion of bronze covered with a CuCl patina, Corros. Sci. 97 (2015) 89–99, https://doi.org/10.1016/j.corsci.2015.04.018.
[17] E. Bernardi, C. Chiavari, B. Lenza, C. Martini, L. Morselli, F. Ospitali, et al., The atmospheric corrosion of quaternary bronzes: the leaching action of acid rain, Corros. Sci. 51 (2009) 159–170, https://doi.org/10.1016/j.corsci.2008.10.008.
[18] L.I. McCann, K. Trentelman, T. Possley, B. Golding, Corrosion of ancient Chinese bronze money trees studied by Raman microscopy, J. Raman Spectrosc. 30 (1999) 121–132, https://doi.org/10.1002/(SICI)1097-4555(199902)30:2<121::AID-JRS355>3.0.CO;2-L.
[19] W. Martens, R.L. Frost, J.T. Kloprogge, P.A. Williams, Raman spectroscopic study of the basic copper sulphates – implications for copper corrosion and 'bronze disease', J. Raman Spectrosc. 34 (2003) 145–151, https://doi.org/10.1002/jrs.969.
[20] V. Hayez, J. Guillaume, A. Hubin, H. Terrin, Micro-Raman spectroscopy for the study of corrosion products on copper alloys: setting up of a reference database and studying works of art, J. Raman Spectrosc. 35 (2004) 732–738, https://doi.org/10.1002/jrs.1194.
[21] W.S. Mokritzky, M. Tatol, Colour difference Delta E - a survey, Mach. Graph. Vis. 20 (2011) 383–412.